Maltose facilitates *Salmonella* growth under nitrogen stress while impairing adhesion to epithelial cells

Kirti Parmar[1], Jayashree S[1], Muralidhar Nayak M[2], Kapudeep Karmakar[3], Sumanta Bagchi[2], Dipshikha Chakravortty[1,4*]

[1]Department of Microbiology and Cell Biology, Division of Biological Sciences, Indian Institute of Science, Bangalore, India.

[2]Centre for Ecological Sciences, Division of Biological Sciences, Indian Institute of Science, Bangalore, India.

[3]Regional Research Station, Terai Zone, Uttar Banga Krishi Viswavidayalaya, Pundibari, Coochbehar, West Bengal, India.

[4]Adjunct Faculty, School of Biology, Indian Institute of Science Education and Research, Thiruvananthapuram, India.

Corresponding author: Prof. Dipshikha Chakravortty

Email: dipa@iisc.ac.in

Abstract

The composition of nutrients in the intestine defines a niche for colonising gut pathogens. The lack of nutrients suitable for pathogens due to competition from resident intestinal microbiota or dietary preferences leads to colonisation failure by pathogens. In this study, we examined the role of the sugar maltose in *Salmonella* Typhimurium (STM) growth under nitrogen-deficient conditions and the pathogenicity of *Salmonella* in the early phases of infection in C57BL/6 mice and colon carcinoma cells (Caco-2 cells). Bacteria grown under nitrogen-deficient conditions with maltose supplementation showed enhanced growth with reduced *Salmonella* pathogenicity island 1 (SPI-1) expression, leading to reduced invasion of Caco-2 cells and reduced organ burden in C57BL/6 mice. Even without nitrogen starvation,

maltose supplementation at lower concentrations inhibited STM colonisation in the ileum of mice. In the cell line model, deleting the maltose metabolism gene (*malQ*) leads to increased adhesion due to increased expression of type 1 fimbriae. We propose that maltose modulates *Salmonella* survival by aiding growth under nitrogen-deficient conditions, and it is detrimental to bacterial infection in epithelial cells.

Introduction –

Food-borne pathogens encounter various stresses inside and outside the host (*1*). Food-borne pathogen growth often occurs in an environment with limited nutrients inside the host owing to competition from resident intestinal microbiota in the host intestine (*2*). Bacteria such as *Salmonella* can successfully modulate their metabolism according to the availability of nutrients. *Salmonella enterica* serovar Typhimurium causes self-limiting gastroenteritis in humans and causes bacteraemia in immunocompromised individuals (*3*).

Successful *Salmonella* colonisation depends on utilising multiple carbon sources, including glycerol, fatty acids, N-acetylglucosamine, gluconate, glucose, lactate, and arginine (*4*). Maltose and maltodextrins are also commonly present carbohydrate sources in the intestine and play pivotal roles in bacterial growth and pathogenesis of different bacteria, both beneficial and detrimental. Compared with glucose, sugars such as maltose/maltodextrins are preferred for growth on poor nitrogen sources (*5*). Maltodextrins promote *Salmonella* survival in the bone marrow-derived macrophages by reducing NADPH expression and recruitment to the SCV. *In vivo*, maltodextrins degrade the intestinal mucosa of mice, increasing the cecal load (*6*). The utilisation of maltose is also crucial for colonisation of the mouse intestine by *E.coli (7)*.

In contrast, maltose derivatives reduce the biofilm production and adhesion of *Pseudomonas aeruginosa* non-swarming mutants (*8*). In zebrafish, maltose modulates immunity against

Vibrio alginolyticus by increasing lysozyme activity and expression (*9*). Lastly, in *Vibrio cholerae*, maltose inhibits cholera toxin secretion and reduces pathogenicity in newborn mice (*10*). These observations highlight the diverse roles of maltose and maltodextrin in bacterial growth and pathogenesis. However, it is still unclear how a carbohydrate, maltose, affects *Salmonella's* virulence factors and provides a growth advantage under nitrogen-deficient conditions. A strain deficient in the maltose hydrolysis gene (*malQ*) was constructed further to study the link between maltose metabolism and virulence. This study aimed to understand the modulation of *Salmonella* virulence and growth with respect to maltose metabolism.

Results

Maltose in nitrogen-free media improves the growth of *Salmonella.*

A Burk medium commonly used to isolate diazotrophs that increase nitrogen in soil was used to evaluate the growth of *Salmonella* in nitrogen-free media (*11*). To validate that our system was nitrogen-free, we performed elemental analysis using Burk's medium, maltose and LB media. Maltose had no traceable amounts of nitrogen, whereas 0.2 - 0.4% nitrogen in Burk's media compared to 8 – 10% in LB media **(Supplementary Figure 1A).** A spectroscopic analysis of the optical density of Burk's medium, which contained varying concentrations of glucose and maltose, was performed. *Salmonella* growth in nitrogen-deficient media was poor and significantly enhanced when supplemented with 0.2% maltose **(Supplementary Figure 1B).** Thus, it was concluded that 0.2% maltose yielded the best growth under nitrogen-deficient conditions. This concentration was used in further experiments. Upon performing a growth curve analysis of *Salmonella* Typhimurium (STM) in four different conditions- Burk's medium (B), Burk's media+ 0.2% maltose (BM), Burk's media+ 0.2% maltose+ 10mM ammonium chloride (BMN), and LB media. We observed luxuriant growth

in nutrient-rich LB media, as expected, and weak growth in Burk's medium (B). There was increased growth in maltose supplementation (BM), but there was no significant advantage in adding nitrogen to BM **(Figure 1A).** In the literature, 10mM ammonium chloride is defined as a nitrogen-rich condition (*12*). CFU growth analysis was performed at different time points to determine the effect of nitrogen on bacterial growth in a nitrogen-deficient medium with maltose (BM). We observed that adding nitrogen (10 mM ammonium chloride) to media supplemented with 0.2% maltose provided a growth advantage only at the initial time point of 3 hours **(Figure 1B).** Nitrogen deficiency in bacteria is indicated by enrichment of metabolite alpha-ketoglutarate and reduced glutamine (*13*). Upon analysis of alpha-ketoglutarate levels in bacteria grown under different conditions mentioned above. It was observed that with increased growth of *Salmonella* in Burk's media+ 0.2% maltose (BM), there were significantly higher alpha-ketoglutarate levels from bacteria grown in the Burk's and LB media. Alpha-ketoglutarate levels were reduced by adding Nitrogen to BM, but not significantly (BMN) **(Figure 1C).**

Bacteria respond to nitrogen deficiency by remodelling gene expression. Nitrogen stress is sensed by proteins GlnB and GlnK of the PII signalling family(*14*), leading to the activation of nitrogen regulatory protein C(NtrC) (*15*). GlnK is essential for bacterial cell viability, colony size and recovery from nitrogen starvation, as deletion causes an inability to regulate nac expression(*16*). Activation of NtrC leads to the increased expression of nitrogen transporters in *E.coli*, resulting in nitrogen influx(4). NtrC also activates *relA*, which couples the nitrogen stress response with the stringent response. Stringent responses lead to metabolically inactive cells or persister cell formation, leading to resistance to antibiotics such as ciprofloxacin(*17-20*). Deletion of the global nitrogen regulator (STM Δ*ntrB*) showed no growth defects in nitrogen-free media supplemented with maltose (BM). However, upon nitrogen supplementation in nitrogen-free media with maltose (BMN), STM Δ*ntrB* showed

an increased lag phase compared to STM WT **(Figure 1D).** The increased lag phase of STM Δ*ntrB* may be due to a defective two-component system responsible for sensing and responding to nitrogen levels.

NtrC also binds to the promoter of eukaryote-like serine-threonine kinase *yeaG* in *E.coli*, which controls population heterogeneity and deletion, leading to compromised survival during prolonged nitrogen starvation owing to its influence of the general stress response regulator RpoS (*21*). RpoS is also required to maintain CFU in *E.coli* during nitrogen starvation (*22*). Increased growth of STM Δ*rpoS* was observed with maltose (BM) compared to WT after 10 hours. Nitrogen supplementation (BMN) did not provide any growth advantage to any strains. At the same time, there was a reduction in nutrient-rich LB media growth of STMΔ*rpoS* **(Figure 1D and supplementary Figure 1C)**. This increased growth of STM Δ*rpoS* in Burk medium with maltose (BM) could be explained by the increased frequency of *rpoS* mutation on glucose limitation, and *rpoS* mutation promotes the growth of bacteria on alternative carbon sources (*23*). RpoE is an alternative sigma factor responsible for maintaining the membrane integrity. We hypothesised that it may be required for survival under nitrogen-deficient conditions. However, STM Δ*rpoE* showed no growth defects in BM and LB media. Its growth was similar to that of the *ntrB* deleted strain. It showed an increased lag phase in nitrogen-free media with maltose and Nitrogen (BMN) conditions **(Figure 1D and supplementary Figure 1C).**

Furthermore, to validate that the increased growth of *Salmonella* in nitrogen-free media when supplemented with maltose (BM) is due to maltose uptake and metabolism, the maltose metabolism gene (*malQ)*, and transporters of maltose (*malEFG*- ABC transporter, *lamB*-maltoporin) were deleted. On the analysis of the growth of these strains in the Burk's media+ 0.2 % maltose (BM), we observed that STM Δ*malQ* and STM Δ*malEFG* showed a significant reduction in growth **(Supplementary Figure 2A, 2B).** In conclusion, maltose

supplementation aids the growth of *Salmonella* in nitrogen-deficient Burk's medium, and RpoS serves as a negative growth regulator.

Salmonella grown in a nitrogen-deficient condition is defective in pathogenesis.

Metabolism is intricately linked with the virulence of pathogens. To analyse the effect on the pathogenesis of *Salmonella* grown in nitrogen-free media when supplemented with maltose (BM) and nitrogen supplementation in nitrogen-free media with maltose (BMN) conditions compared to the nutrient LB media. It was observed that invasion of STM WT was significantly reduced when grown in BM (Burk+ maltose) and BMN(Burk+ maltose + ammonium chloride) in Caco2 cells **(Figure 2A).** *Salmonella* invasion depends on *Salmonella* pathogenicity island 1 (SPI-1) effectors secreted into host cells, leading to the cytoskeletal arrangement (*24*). Upon q-RT PCR analysis of the SPI-1 genes (*sipB, invF* and *hilA*), it was observed that *Salmonella* grown in BM and BMN media had downregulated these genes compared to those grown in LB. *hilA,* the transcriptional regulator of SPI-1, was downregulated in *Salmonella* grown in Burk+maltose (BM) compared to Burk+ maltose + ammonium chloride (BMN) **(Figure 2B).** In the *in-vivo* pathogenesis model in C57BL/6 male mice, we observed that *Salmonella* grown in BM (Burk+ maltose) was less pathogenic than the other three conditions (B, BMN and LB). There was also less weight reduction in mice infected with BM-grown *Salmonella* **(Figure 2C).** These mice survived longer than those fed with *Salmonella* grown in B, BMN and LB **(Figure 2D).** Furthermore, the organ burden in C57BL/6 mice infected with BM-grown *Salmonella* was reduced in blood, mesenteric lymph nodes (MLN), liver and spleen compared to LB-grown *Salmonella* five days post-infection **(Figure 2E).**

The absence of maltose metabolism increases invasion and adhesion.

The defect in the pathogenesis observed in the BM-grown *Salmonella* could be due to growth in nitrogen-deficient conditions, or maltose might act as an inhibitory molecule. It has been reported in the literature that colonising mice with simple sugars utilised by intestinal microbiota decreases the pathogen burden by competing with the pathogen for that sugar (*25*). To answer this question, the C57BL/6 mice were treated with various concentrations of maltose, and it was observed that at 1% maltose treatment, STM WT infection was reduced in the ileum at 24 hours **(Figure 3A).** This inhibition was not observed at higher maltose concentrations. Maltose metabolism has been reported to reduce bacterial colonisation from the third-day post-infection(*7*). Similar to earlier studies, it was observed that STM Δ*malQ* showed colonisation defects in blood, MLN, liver and spleen compared to STM WT at 5 days post-infection **(Supplementary Figure 3).** However, STM Δ*malEFG* showed no growth defect in colonising various mice organs.

To further study the role of maltose in *Salmonella* infection., on infection of Caco2 cells, to our surprise, there was an increased invasion in colon carcinoma (Caco-2) cells of STMΔ*malQ,* which is reduced upon complementation of the *malQ* gene. In contrast, the maltose transporter (*malEFG)* deletion did not affect the invasion compared to STM WT **(Figure 3B).** Increased invasion of STM Δ*malQ* was present under both conditions in nitrogen-free media when supplemented with maltose (BM) grown and LB-grown compared to STM WT. Further experiments were performed using LB-grown bacteria. Adhesion to host cells is the first step in facilitating the invasion and colonisation of the host. *Salmonella* adhesion depends on various fimbriae and adhesins secreted by the type 1(BapA and SiiE) and type 5 (MisL, ShdA and SadA) secretion systems. Large outer membrane proteins such as PagN and Rck also help in adhesion (*26*). We further examined the adhesion of the *malQ* deleted strain and observed an increased adhesion of Caco2 cells **(Figure 3C).** Upon investigating the mRNA expression of various factors responsible for the invasion and

adhesion in the *malQ* deleted strain compared to STM WT by qRT-PCR. It was observed that SPI-1 genes (*hilA*, i*nvF, sipA)* responsible for the invasion were downregulated in STM Δ*malQ* compared to STM WT. In the literature, it has been shown that invasion of Caco2 cells is largely independent of SPI-1, PagN and RcK. The triple knock-out of these genes could invade only slightly less than the WT (*27*). Next, upon investigation of the adhesion genes- encoding large proteins *pagN, ompD* were downregulated, whereas *siiE* and *fimA* were upregulated in STM Δ*malQ* ***(*****Figure 3D).** *siiE* has been reported to play a role in the adhesion only in polarised Caco 2 cells (*28*). *fimA* is a major structural protein of the type 1 fimbriae that mediates adhesion. Upon visualisation of type 1 fimbriae with transmission electron microscopy (TEM), more type 1 fimbriae were observed in STM Δ*malQ* bacteria collected from the overnight culture compared to STM WT. Thus, the deletion of *malQ* increased the type 1 fimbriae production **(Figure 3E).** Thus, we concluded that increased *fimA* might be responsible for the increased adhesion and invasion. Our results are in accordance with the literature, which shows an inverse relation between the expression of SPI-1 and type 1 fimbriae (*29*). The above results prove that the deletion of *malQ* is associated with concomitant increases in the fimbriae production, suggesting the anti-adhesive role of *malQ*.

Increased adhesion is due to the enhancement of type 1 fimbriae.

Type 1 fimbriae bind to host glycoproteins such as mannose using FimH, and incubation with the 0.2 M Mannose can inhibit the binding of *Salmonella* to the host by Type 1 fimbriae (*30*). To elucidate whether the increased adhesion depended on the interaction with mannose residues of the eukaryotic cells, bacteria were incubated for 1 hour before infection with 0.2M mannose. The increased adhesion of the STM Δ*malQ* was significantly reduced by pretreatment with mannose **(Figure 4A).** Confocal microscopy was performed to confirm

further that the increased adhesion in STM Δ*malQ* was due to increased fimbriae. Increased adhesion to Caco2 of STM Δ*malQ* compared to STM WT was observed, which was inhibited by adding mannose **(Figure 4B and 4C).** Type 1 fimbriae have also been reported to facilitate biofilm formation (*31*). The biofilm was grown with various concentrations to determine the role of maltose in biofilm formation. Maltose also acted as an inhibitory signal in biofilm formation. (**Supplementary Figure 4A)**. Furthermore, in the biofilm assay with STM Δ*malQ,* STM Δ*malEFG* and STM Δ*lamB,* it was observed that there was no significant reduction of biofilm in STM Δ*malQ,* STM Δ*malEFG* compared to STM WT (**Supplementary Figure 4B)**. Thus, it suggested that *malQ* and maltose transport into bacteria by *malEFG* mediated the decreased biofilm.

To elucidate the mechanism of STM*Δ malQ* mediated regulation of type1 fimbriae. The mRNA expression levels of type 1 fimbriae regulators (*fimY, fimZ* and *fimW*) were determined. FimY and FimZ positively regulate type 1 fimbriae in *Salmonella*, whereas FimW negatively regulates them. FimZ also represses the expression of SPI-1 via *hilE (32, 33)*. There was no change in the expression of *fimZ,* whereas *fimY* and *fimW* were significantly upregulated in the STM*Δ malQ* **(Figure 4D).** The significantly increased expression of *fimY* might be responsible for the increased production of type 1 fimbriae. Type 1 fimbria in Gram-negative bacteria such as uropathogenic *E.coli* and *Serratia marcescens* are reported to be repressed by the carbohydrate metabolism-regulating system cAMP- CRP *(34, 35).* Upon analysis of the mRNA expression of CRP in STM *ΔmalQ,* we observed significant downregulation compared to STM WT (**Supplementary Figure 5A)**. Thus, the increased type 1 fimbria production in STM *ΔmalQ* was due to increased expression of *fimY,* which might be modulated by the decreased expression of CRP.

Previous reports have shown that *rpoE* may be negatively regulated by cAMP-CRP in *Salmonella(36). rpoE* also regulates the pathogenicity genes of *E.coli* in interaction with

human brain microvascular endothelial cells and the thin aggregative fimbriae(Agf) in *Salmonella* (*37*, *38*). The qRT-PCR analysis of the *rpoE* gene in STM *ΔmalQ* revealed upregulation of *rpoE* compared to STM WT (**Supplementary Figure 5B)**. Upon deletion of *rpoE* in the STM *ΔmalQ* and performing adhesion to Caco2 cells, we observed that increased adhesion of STM *ΔmalQ* was lost. STM Δ*rpoE* had less adhesion than STM WT, and double deletion of *rpoE* and *malQ* resulted in adhesion similar to STM Δ*rpoE* (**Supplementary Figure 5C)**. Thus, the increased adhesion of STM *ΔmalQ* was mediated by the alternative sigma factor RpoE.

Discussion-

In this study, we examined the role of maltose in aiding the growth of *Salmonella* Typhimurium under nitrogen-deficient conditions and modulating virulence by inhibiting the adhesion to eukaryotic cells. The most common bacterium used to study bacterial survival in nitrogen-deficient conditions is *E.coli*, which, upon nitrogen starvation, stops growing abruptly from maximum to zero in 27 minutes (*39*). *E.coli* also had a doubling time of 39 hours during prolonged nitrogen starvation, which is 80-fold higher than the doubling time under nutrient-rich conditions. This growth was attributed to the breakdown of allantoin, which is formed by nucleic acid degradation (*40*). Similarly, peptidoglycan degradation and transport are activated during nitrogen starvation as these tripeptides may serve as a nitrogen source for bacteria (*41*). Previous reports in the literature for mimicking enteric bacteria in nitrogen-deficient conditions have used M9 or Gutnick's minimal media supplemented with 3mM ammonium chloride as a nitrogen source, which eventually runs out during the experiment as compared to 10mM ammonium chloride as a nitrogen-rich condition. Our study found that nitrogen-deficient Burk's media could support—the *g*rowth of *Salmonella* under nitrogen-deficient conditions by adding maltose. Adding external nitrogen source, such

as ammonium chloride provided advantage in the growth only at initial time point of 3 hours. *Salmonella* grown in these conditions had high alpha-ketoglutarate levels, and growth was found to be independent of the NtrBC two-component system. Bacteria grown in nitrogen-deficient conditions were defective in pathogenesis in cell line model Caco2 and *in-vivo* C57BL/6 mice compared to bacteria grown in nutrient-rich LB media.

Maltose utilisation is essential for the survival of the *E.coli* in the mouse intestine as shown by Jones et al. (*7*). As observed earlier, we found no difference in the intestinal colonisation of maltose metabolism mutant STM Δ*malQ* in the mouse's ileum, cecum and faeces after 1-day post-infection. However, decreased ileum colonisation of STM WT was observed in the treatment of 1% maltose in mice. Furthermore, STM Δ*malQ* showed higher invasion and adhesion in the epithelial cells Caco-2. The higher adhesion depended on the higher expression of type 1 fimbriae by STM Δ*malQ*. The Inhibition of adhesion mediated by type 1 fimbria with the addition of mannose reversed the advantage of increased adhesion. As shown by Muller et al., the Carbohydrate metabolism-regulating system cAMP- CRP mediates the type 1 fimbriae expression by *fimB*-mediated recombination in *E.coli*, which is absent in *Salmonella(34)*. Further studies are required to address how the maltose metabolism gene (*malQ)* regulates fimbriae production through cAMP-CRP. The alternative sigma factor *rpoE* is essential for the membrane integrity of bacteria and essential during various stresses faced by bacteria (*42*). RpoE has also been known to induce fimbriae and invasion in *E.coli* (*37*). Deletion of the *rpoE* in STM Δ*malQ* had a similar effect to the addition of mannose and STM Δ*rpoE,* STMΔ*malQ*Δ*rpoE* had similar adhesion. Thus, the increased adhesion of STM ΔmalQ is dependent on *rpoE*. Deletion of *rpoE* induces multiple phenotypes in bacteria, and the exact regulation mechanism by maltose metabolism remains unknown.

Material and Methods-

Bacteria and growth conditions- Wild-type *Salmonella* Typhimurium 14028s (STM WT) was obtained from Profeesor Michael Hensel (Universitat Osnabruck). STM WT was revived from glycerol stock kept at -80°C and streaked on LB-agar; the respective antibiotic-containing plates were used for the knock-out and complement strains. All the bacterial strains were grown in LB supplemented with the required antibiotics at 37°C and 170 rpm overnight. The strain containing pkD46 was grown at 30°C and 170rpm. The growth of the different bacterial strains was measured for 24 hours at 3-hour intervals using absorbance at 600nm and CFU analysis by plating on LB-agar. To mimic the nitrogen-deficient state, Burk's media(hi-media) was used and supplemented with various carbon sources, as well as ammonium chloride. Growth measured using Bioscreen was performed at 1-hour intervals for 24 hours. A list of bacterial strains used in the study is attached in Supplementary Table 1.

Construction of knock-out strains- The gene knock-out strains were prepared using a one one-step chromosomal gene inactivation protocol by Datsenko and Wannner (*43*). In this protocol, knock-out primers were designed 40bp homologous to the gene to be knocked out, and a 20bp extension for the antibiotic cassette was added. The gene coding for the antibiotic is amplified from the pKD3 or pKD4 plasmid, and through homologous recombination, the gene is replaced by an antibiotic cassette using electroporation. Amplified cassettes were inserted into STM pKD46, which has a lambda red recombinase system under an arabinose inducible promoter. For electroporation, STM pKD 46 bacterial cells were grown until log phase, and absorbance of 0.3 and made electrocompetent by washing with MilliQ and 10% glycerol at 4°C. The knock-out strains were screened by plating the bacteria on an antibiotic-

containing plate and PCR of the obtained colonies. The primers used in the study are attached in Supplementary Table 2.

Construction of complement strains- *malQ* gene amplified from the *Salmonella* Typhimurium and pBAD vector were digested with KpnI and PstI at 37°C for 1 hour. Digested products were gel purified and ligated with T4 DNA ligase (NEB). Ligated products were transformed into *E.coli* Tg1 competent cells using the heat shock method. Transformed cells were plated on the LB-chloramphenicol and incubated overnight at 37°C. Plasmid isolation was performed from transformants. Cloning was confirmed by double digestion. After successful confirmation, the clone was transformed into STM Δ*malQ*.

Elemental analysis- To check the nitrogen status, elemental analysis was performed in LB, Burk's medium and maltose to confirm the presence of any nitrogen contamination. Elemental analysis was performed using gas chromatography (Vario EL Cube, Elementar, Germany).

Eukaryotic cell lines and growth conditions- Cell line Caco-2 used in this study was maintained in Dulbecco's Modified Eagle'sMedia (Sigma-Aldrich) supplemented with 10% FBS (fetal bovine serum, Gibco), 1% sodium pyruvate, 1% penicillin-streptomycin, and 1% non-essential amino acids at 37°C in the presence of 5% CO2. Cells were grown to confluence, and after counting them with a haemocytometer, an equal number of cells were seeded into 24 well plates.

Invasion assay- one lakh seeded Caco2 cells were infected with bacteria at an MOI of 10, and a log phase culture was used to infect the epithelial cells(Caco 2 cells). Cells were centrifuged at 800 rpm for 5 min and incubated at 37°C, 5% CO_2 for 25 minutes. Cells were then washed with 1X PBS to remove all the extracellular bacteria, and media containing 100µg/ml gentamicin in DMEM with FBS was added for 1 hour. Similarly, 25 µg/ml of gentamicin in DMEM media with FBS was added, and the cells were incubated until lysis. Cells were lysed with 0.1% of triton X 100 at 2 hours. Bacteria were plated on the LB Agar, incubated at 37°C for 12 hours, and colonies were counted. To calculate the percentage invasion, bacterial CFU at 2 hours was divided by the pre-inoculum CFU.

Adhesion assay – log phase bacteria were adjusted to 0.3 OD and incubated with and without 0.2M Mannose for 1 hour before infection. Caco2 cells were infected with MOI of 10 and incubated for 10 minutes. Cells were washed with 1X PBS and lysed using 0.1%triton X 100. Bacteria were plated on the LB Agar and incubated at 37°C for 12 hours, and colonies were counted. The number of adhered cells was calculated by dividing the obtained CFU with Pre-inoculum values of the bacteria used for infection. The cells were seeded with coverslips for confocal microscopy, and the assay mentioned above was performed. At the endpoint, the cells were fixed using 3.5% Paraformaldehyde for 10 min, followed by washing with 1xPBS and storing samples in 1x PBS.

Confocal microscopy- The PFA fixed samples from the adhesion assay were stained with primary antibody against *Salmonella* (1:500 in 2.5% BSA) overnight at 4°C. The primary antibody was washed with 1xPBS, and the secondary antibody was added for 45 minutes at room temperature. Samples were then stained with FM-464 for 10 minutes and given one

final wash. Coverslips were mounted on the slides after adding the mounting media and sealed.

Percentage adhesion was calculated by dividing the number of bacteria by the number of Caco2 cells in the acquired images. Images were acquired using a Zeiss 880 confocal microscope and analysed by Zeiss Zen Black 2012 software.

Biofilm formation- Bacteria were grown until the stationary phase, inoculated in biofilm media(tryptone and yeast extract) with different concentrations of maltose, and incubated at 28°C for 3 days. The biofilm formed was measured using crystal violet staining, and the absorbance was measured at 570 nm.

Alpha-ketoglutarate estimations- A protocol from Rabinowitz et al. was followed (*44*). Briefly, STM WT bacteria were grown overnight in different conditions, as mentioned in the data and harvested at 5,000 rpm for 5 min. Acetonitrile extraction was performed by adding acetonitrile, water and formic acid (0.1M) containing extraction solvent in an 80:20 ratio. Samples were incubated at -20°C for 15 minutes and then centrifuged at 13000 rpm, 4°C to separate insoluble materials from the extracted metabolites. The resulting pellet was reextracted twice using the same solvent at 4 °C. The alpha ketoglutaric acid standard was prepared by dissolving it in MQ. All the samples were analysed by mass spectroscopy and concentration of alpha-ketoglutarate was determined. The Obtained values were then normalised to the CFU of bacteria in the sample.

UPLC Conditions and ESI-Triple quad Mass Spectrometry

The sample extracts were analysed using a UPLC – ESI – MS/MS system (UPLC, SHIMADZU, LCMS-8045) with lab solution software. The UPLC conditions are described

as follows: Mobile phase A: water containing 0.1% Formic acid, Mobile phase B: Methanol with an isocratic elution of 50% mobile phase A and 50% mobile phase B with a Flow rate of 0.5mL/ min. The injection volume used is 50µl with a total run time of 2min. Column temperature is 25°C and Autosampler temperature is 15°C. The ESI source parameters were set: ion spray voltage 4000 V (positive ion mode); other set parameters were interface temperature 300 °C, Desolvation temperature 526 °C, Nebulizing gas flow rate 3 L/min, Dry gas flow rate 10L/min, Heating gas flow rate of 10L/min, Heat block temperature 400 °C, CID gas (Argan gas 99.9995% for collision) flow limit set to 230kPa. Then, the ion reaction monitoring (MRM) mode was selected using mass spectrometry scanning, and the specific mass-to-charge ratio (m/z) of Alpha ketoglutaric acid (145.05m/z) was then set using QQQ scans in MRM mode. The precursor ion, 145.05m/z and product ion, 101.00m/z, are selected for ion section transfer by a Based Peak Intensity (BPI) scan. Operational parameters such as ion source gas, scan time, and collision energy are set to obtain optimal signal intensity and peak separation. Each scan event time was set to 0.309 sec.

RNA isolation and cDNA Synthesis- The bacterial culture was pelleted down by centrifugation at 6000 rpm for 10 min, and 1 ml of TRIzol was added to the pellet. Samples were kept at -80°C till the time they were processed. The lysed supernatant was extracted with chloroform, and RNA precipitation was done using an equal volume of isopropanol. The obtained pellet was washed with 70% ethanol in DEPC water and air-dried. The RNA was dissolved in DEPC water. The quality and quantity of RNA were checked using Nanodrop and 2% agarose gel electrophoresis.

DNase treatment(Thermo Fisher Scientific) was performed on the isolated RNA at 37°C for 1 hour, followed by heat inactivation at 65°C for 15 minutes. DNase-treated RNA was

converted to cDNA using the Primescript Reagent RT kit (Takara). Q-RT PCR was performed using the TB green RT-qPCR Kit in a real-time PCR system.

For analysis of RT data, 16s rRNA was used as the reference gene to calculate the dct of the samples. ddct was calculated by comparing two different samples.

Animal experiments- All the animal experiments were approved by the Institutional Animal Ethics Committee (IAEC), Indian Institute of Science, Bangalore. The ethical clearance number for this study was CAF/ethics/852/ 2021. All the animals were acquired from the central animal facility at the Indian Institute of Science, Bangalore.

5-6 weeks old C57BL/6 male mice were used for survival and organ burden determination. Mice were orally gavaged with 10^{8} (100µL)bacteria, and their weight health was monitored to calculate their weight reduction percentage and survival rate. To determine the organ burden in mice, mice were orally gavaged with 10^{7}(100µL) bacteria, euthanised, and various mice organs (Blood, Liver, MLN, spleen, ileum) were acquired. Blood was isolated by performing a heart puncture. Mouse organs were homogenised and plated on *Salmonella Shigella* agar to determine the bacterial burden in various organs.

TEM- Transmission electron microscopy was performed according to a previously described protocol (*45*). Stationery and log phase cultures of STM WT and STM *ΔmalQ* were washed twice with 1X PBS and resuspended in 50 µL of 1X PBS. 5 µL of the sample was placed on the copper grids. After air drying, samples were negatively stained with 1% uranyl acetate. TEM microscopy was performed using a JEM-100 CX II; JEOL.

Statistics- The Statistical tests used in the experiments are mentioned in the figure legends. For the animal experiments, the Mann- Whitney test was performed. All the data were plotted and analysed by using GraphPad Prism 8.

Acknowledgements

Dr Abhilash Vijay Nair is acknowledged for helping with the oral gavage of the animals. We acknowledge the department's Real-time facility, confocal microscopy facility and central animal facility at IISc for supporting the experiments. Professor Sumanta Bagchi acknowledges DST(FIST) for the elemental analysis instrument. We sincerely thank Amit Sahu and Niladri for their help with the growth curve machine (Bioscreen).

Funding

This work was funded by the DAE SRC fellowship and the DBT-IISc partnership program for advanced research in biological sciences and Bioengineering to DC. We acknowledge the infrastructure support from ICMR (Centre for Advanced Study in Molecular Medicine), DST (FIST), TATA fellowship and UGC (special assistance). KP sincerely acknowledges IISc-MHRD for the fellowship. The funders played no role in the study design, data collection, analysis, or manuscript writing.

Author contributions

KP- writing- review and editing, visualisation, experimental design, investigation and data analysis. **Js-** Investigation. **KK-** manuscript editing and visualisation, **MN**-alpha-ketoglutarate estimations. **SB**- elemental analysis. **DC**- writing- review and editing, visualisation, experimental design, investigation, data analysis, resources and supervision.

Declaration of interest

The authors declare no conflict of interest.

Data and material availability

All the data are available in the main text or the supplementary file.

References

1. M. D. Winfield, E. A. Groisman, Role of nonhost environments in the lifestyles of Salmonella and Escherichia coli. *Appl Environ Microbiol* **69**, 3687-3694 (2003).
2. G. Caballero-Flores, J. M. Pickard, G. Nunez, Microbiota-mediated colonization resistance: mechanisms and regulation. *Nat Rev Microbiol* **21**, 347-360 (2023).
3. J. A. Crump *et al.*, Nontyphoidal Salmonella Invasive Disease: Challenges and Solutions. *Open Forum Infect Dis* **10**, S32-S37 (2023).
4. B. Steeb *et al.*, Parallel exploitation of diverse host nutrients enhances Salmonella virulence. *PLoS Pathog* **9**, e1003301 (2013).
5. A. Bren *et al.*, Glucose becomes one of the worst carbon sources for E.coli on poor nitrogen sources due to suboptimal levels of cAMP. *Sci Rep* **6**, 24834 (2016).
6. K. P. Nickerson *et al.*, The dietary polysaccharide maltodextrin promotes Salmonella survival and mucosal colonization in mice. *PLoS One* **9**, e101789 (2014).
7. S. A. Jones *et al.*, Glycogen and maltose utilization by Escherichia coli O157:H7 in the mouse intestine. *Infect Immun* **76**, 2531-2540 (2008).
8. G. S. Shetye *et al.*, Specific maltose derivatives modulate the swarming motility of nonswarming mutant and inhibit bacterial adhesion and biofilm formation by Pseudomonas aeruginosa. *Chembiochem* **15**, 1514-1523 (2014).
9. M. Jiang *et al.*, Exogenous maltose enhances Zebrafish immunity to levofloxacin-resistant Vibrio alginolyticus. *Microb Biotechnol* **13**, 1213-1227 (2020).
10. H. Lang, G. Jonson, J. Holmgren, E. T. Palva, The maltose regulon of Vibrio cholerae affects production and secretion of virulence factors. *Infect Immun* **62**, 4781-4788 (1994).
11. M. Park *et al.*, Isolation and characterization of diazotrophic growth promoting bacteria from rhizosphere of agricultural crops of Korea. *Microbiol Res* **160**, 127-133 (2005).
12. J. Schumacher *et al.*, Nitrogen and carbon status are integrated at the transcriptional level by the nitrogen regulator NtrC in vivo. *mBio* **4**, e00881-00813 (2013).
13. S. Pierzynowski, K. Pierzynowska, Alpha-ketoglutarate, a key molecule involved in nitrogen circulation in both animals and plants, in the context of human gut microbiota and protein metabolism. *Adv Med Sci* **67**, 142-147 (2022).
14. K. Forchhammer, J. Luddecke, Sensory properties of the PII signalling protein family. *FEBS J* **283**, 425-437 (2016).

15. A. Switzer, D. R. Brown, S. Wigneshweraraj, New insights into the adaptive transcriptional response to nitrogen starvation in Escherichia coli. *Biochem Soc Trans* **46**, 1721-1728 (2018).
16. T. A. Blauwkamp, A. J. Ninfa, Physiological role of the GlnK signal transduction protein of Escherichia coli: survival of nitrogen starvation. *Mol Microbiol* **46**, 203-214 (2002).
17. S. Iyer, D. Le, B. R. Park, M. Kim, Distinct mechanisms coordinate transcription and translation under carbon and nitrogen starvation in Escherichia coli. *Nat Microbiol* **3**, 741-748 (2018).
18. H. B. Sanchuki *et al.*, Dynamics of the Escherichia coli proteome in response to nitrogen starvation and entry into the stationary phase. *Biochim Biophys Acta Proteins Proteom* **1865**, 344-352 (2017).
19. D. R. Brown, Nitrogen Starvation Induces Persister Cell Formation in Escherichia coli. *J Bacteriol* **201**, (2019).
20. D. R. Brown, G. Barton, Z. Pan, M. Buck, S. Wigneshweraraj, Nitrogen stress response and stringent response are coupled in Escherichia coli. *Nat Commun* **5**, 4115 (2014).
21. R. Figueira *et al.*, Adaptation to sustained nitrogen starvation by Escherichia coli requires the eukaryote-like serine/threonine kinase YeaG. *Sci Rep* **5**, 17524 (2015).
22. M. S. Kabir *et al.*, Effects of mutations in the rpoS gene on cell viability and global gene expression under nitrogen starvation in Escherichia coli. *Microbiology (Reading)* **150**, 2543-2553 (2004).
23. L. Notley-McRobb, T. King, T. Ferenci, rpoS mutations and loss of general stress resistance in Escherichia coli populations as a consequence of conflict between competing stress responses. *J Bacteriol* **184**, 806-811 (2002).
24. D. Hajra, A. V. Nair, D. Chakravortty, An elegant nano-injection machinery for sabotaging the host: Role of Type III secretion system in virulence of different human and animal pathogenic bacteria. *Phys Life Rev* **38**, 25-54 (2021).
25. N. Kamada *et al.*, Regulated virulence controls the ability of a pathogen to compete with the gut microbiota. *Science* **336**, 1325-1329 (2012).
26. C. Wagner, M. Hensel, Adhesive mechanisms of Salmonella enterica. *Adv Exp Med Biol* **715**, 17-34 (2011).
27. S. M. Roche *et al.*, Salmonella Typhimurium Invalidated for the Three Currently Known Invasion Factors Keeps Its Ability to Invade Several Cell Models. *Front Cell Infect Microbiol* **8**, 273 (2018).
28. M. Lorkowski, A. Felipe-Lopez, C. A. Danzer, N. Hansmeier, M. Hensel, Salmonella enterica invasion of polarized epithelial cells is a highly cooperative effort. *Infect Immun* **82**, 2657-2667 (2014).
29. S. Saini, J. M. Slauch, P. D. Aldridge, C. V. Rao, Role of cross talk in regulating the dynamic expression of the flagellar Salmonella pathogenicity island 1 and type 1 fimbrial genes. *J Bacteriol* **192**, 5767-5777 (2010).
30. D. Kisiela *et al.*, Functional characterization of the FimH adhesin from Salmonella enterica serovar Enteritidis. *Microbiology (Reading)* **152**, 1337-1346 (2006).
31. J. D. Boddicker, N. A. Ledeboer, J. Jagnow, B. D. Jones, S. Clegg, Differential binding to and biofilm formation on, HEp-2 cells by Salmonella enterica serovar Typhimurium is dependent upon allelic variation in the fimH gene of the fim gene cluster. *Mol Microbiol* **45**, 1255-1265 (2002).
32. S. Saini, J. A. Pearl, C. V. Rao, Role of FimW, FimY, and FimZ in regulating the expression of type i fimbriae in Salmonella enterica serovar Typhimurium. *J Bacteriol* **191**, 3003-3010 (2009).
33. M. A. Baxter, B. D. Jones, The fimYZ genes regulate Salmonella enterica Serovar Typhimurium invasion in addition to type 1 fimbrial expression and bacterial motility. *Infect Immun* **73**, 1377-1385 (2005).

34. C. M. Muller *et al.*, Type 1 fimbriae, a colonization factor of uropathogenic Escherichia coli, are controlled by the metabolic sensor CRP-cAMP. *PLoS Pathog* **5**, e1000303 (2009).
35. E. J. Kalivoda, N. A. Stella, D. M. O'Dee, G. J. Nau, R. M. Shanks, The cyclic AMP-dependent catabolite repression system of Serratia marcescens mediates biofilm formation through regulation of type 1 fimbriae. *Appl Environ Microbiol* **74**, 3461-3470 (2008).
36. H. Miticka *et al.*, Transcriptional analysis of the rpoE gene encoding extracytoplasmic stress response sigma factor sigmaE in Salmonella enterica serovar Typhimurium. *FEMS Microbiol Lett* **226**, 307-314 (2003).
37. Y. Fan, J. Bai, D. Xi, B. Yang, RpoE Facilitates Stress-Resistance, Invasion, and Pathogenicity of Escherichia coli K1. *Microorganisms* **10**, (2022).
38. A. Y. Yoo *et al.*, Role of sigma factor E in regulation of Salmonella Agf expression. *Biochem Biophys Res Commun* **430**, 131-136 (2013).
39. A. Bren, Y. Hart, E. Dekel, D. Koster, U. Alon, The last generation of bacterial growth in limiting nutrient. *BMC Syst Biol* **7**, 27 (2013).
40. A. Switzer, L. Burchell, J. McQuail, S. Wigneshweraraj, The Adaptive Response to Long-Term Nitrogen Starvation in Escherichia coli Requires the Breakdown of Allantoin. *J Bacteriol* **202**, (2020).
41. U. Choi, Y. H. Park, Y. R. Kim, Y. J. Seok, C. R. Lee, Increased expression of genes involved in uptake and degradation of murein tripeptide under nitrogen starvation in Escherichia coli. *FEMS Microbiol Lett* **363**, (2016).
42. J. D. Hayden, S. E. Ades, The extracytoplasmic stress factor, sigmaE, is required to maintain cell envelope integrity in Escherichia coli. *PLoS One* **3**, e1573 (2008).
43. K. A. Datsenko, B. L. Wanner, One-step inactivation of chromosomal genes in Escherichia coli K-12 using PCR products. *Proc Natl Acad Sci U S A* **97**, 6640-6645 (2000).
44. J. D. Rabinowitz, E. Kimball, Acidic acetonitrile for cellular metabolome extraction from Escherichia coli. *Anal Chem* **79**, 6167-6173 (2007).
45. S. A. Marathe *et al.*, Curcumin Reduces the Motility of Salmonella enterica Serovar Typhimurium by Binding to the Flagella, Thereby Leading to Flagellar Fragility and Shedding. *J Bacteriol* **198**, 1798-1811 (2016).
46. D. Mukherjee, D. Chakravortty, A Tale of Twins: The Distinct Roles of Intracellular and Extracellular Formate in Regulating Flagellar and Pathogenicity Island-1 Genes in Salmonella Typhimurium. 2024.2001.2030.577997 (2024).

Main figure legends

Figure 1. *Salmonella* growth in a nitrogen-deficient medium was enhanced by maltose supplementation.

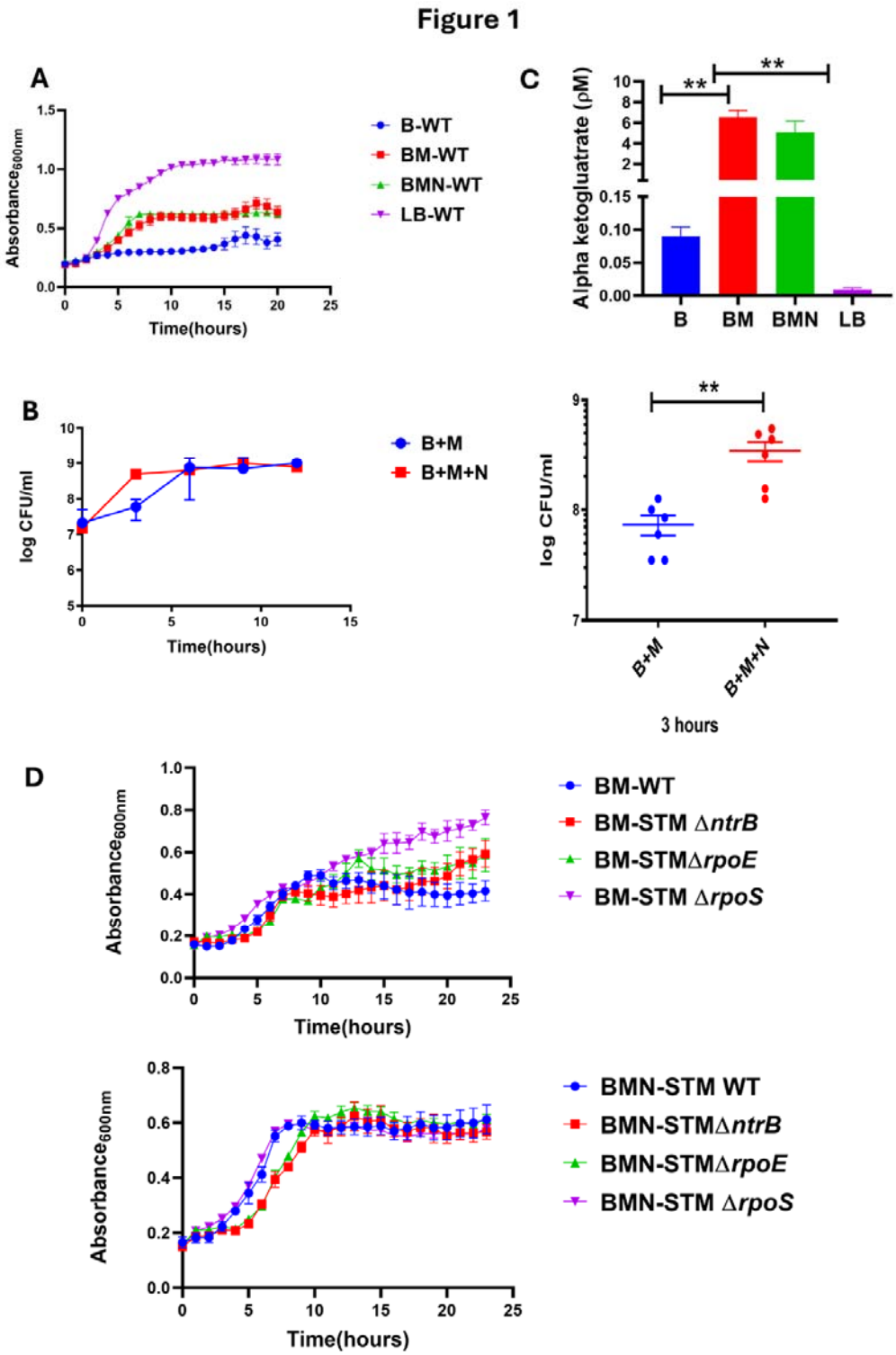

A. Growth curve analysis by absorbance of STM WT grown under four different conditions at various time points. Media conditions- B (Burk's medium), BM (Burk's medium + 0.2% maltose), BMN (Burk's medium + 0.2% maltose +10mM ammonium chloride), LB (Luria Bertini medium). Data are representative of N=3,n=5, presented as mean±SD.

B. Growth curve analysis by CFU of STM WT grown in BM and BMN at various time points. Statistical analysis of growth at 3-hour time point was performed using an unpaired Student's t-test. Data are representative of N=3,n=2, presented as mean ±SEM.

C. Estimation of alpha-ketoglutarate levels in STM WT grown in four different conditions mentioned above. Statistical analysis was performed by using an unpaired Student's t-test. N=2, presented as mean±SEM.

D. Growth curve analysis by absorbance of STM WT, STM Δ*ntrB,* STM Δ*rpoE, and* STM Δ*rpoS* under BM and BMN conditions at various time points. Data are representative of N=3, n=5, presented as mean±SD.

Figure 2. *Salmonella* grown in the nitrogen-deficient condition is attenuated in the pathogenesis

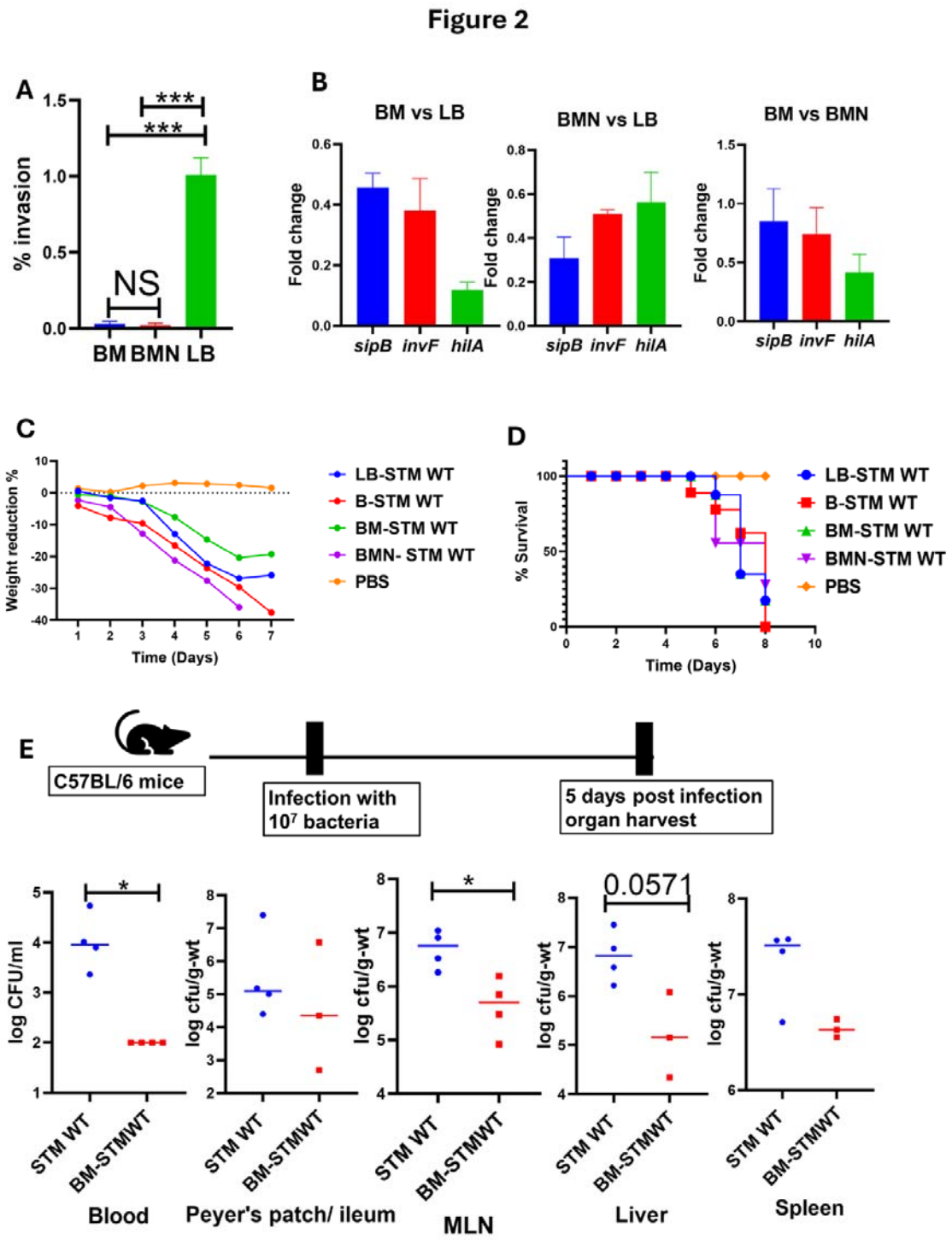

A. Percentage invasion of STM WT grown under different conditions - BM (Burk's medium + 0.2% maltose), BMN (Burk's medium + 0.2% maltose +10mM ammonium chloride), LB (Luria Bertini medium). Unpaired Student's t-test was used for analysis. Data are representative of N=4, n=3, presented as mean ±SEM.

B. mRNA expression of SPI-1 genes (*sipB, invF* and *hilA)* by q-RT PCR in BM, BMN and LB media grown STM WT. Data are representative of N=3, n=3, presented as mean ±SD.

C and D. Weight reduction percentage and survival in C57BL/6 mice post infection by STM WT grown in B, BM, BMN and LB media. Five animals per cohort were used for the survival curve.

E. Schematic representation of infection for organ burden determination of STM WT grown in BM and LB. Organ burden in blood, peyer's patches, MLN, liver and spleen. The Mann- Whitney test was performed for the analysis—five animals per cohort were presented as mean ±SD.

Figure 3. *malQ* deletion increases *Salmonella* invasion and adhesion.

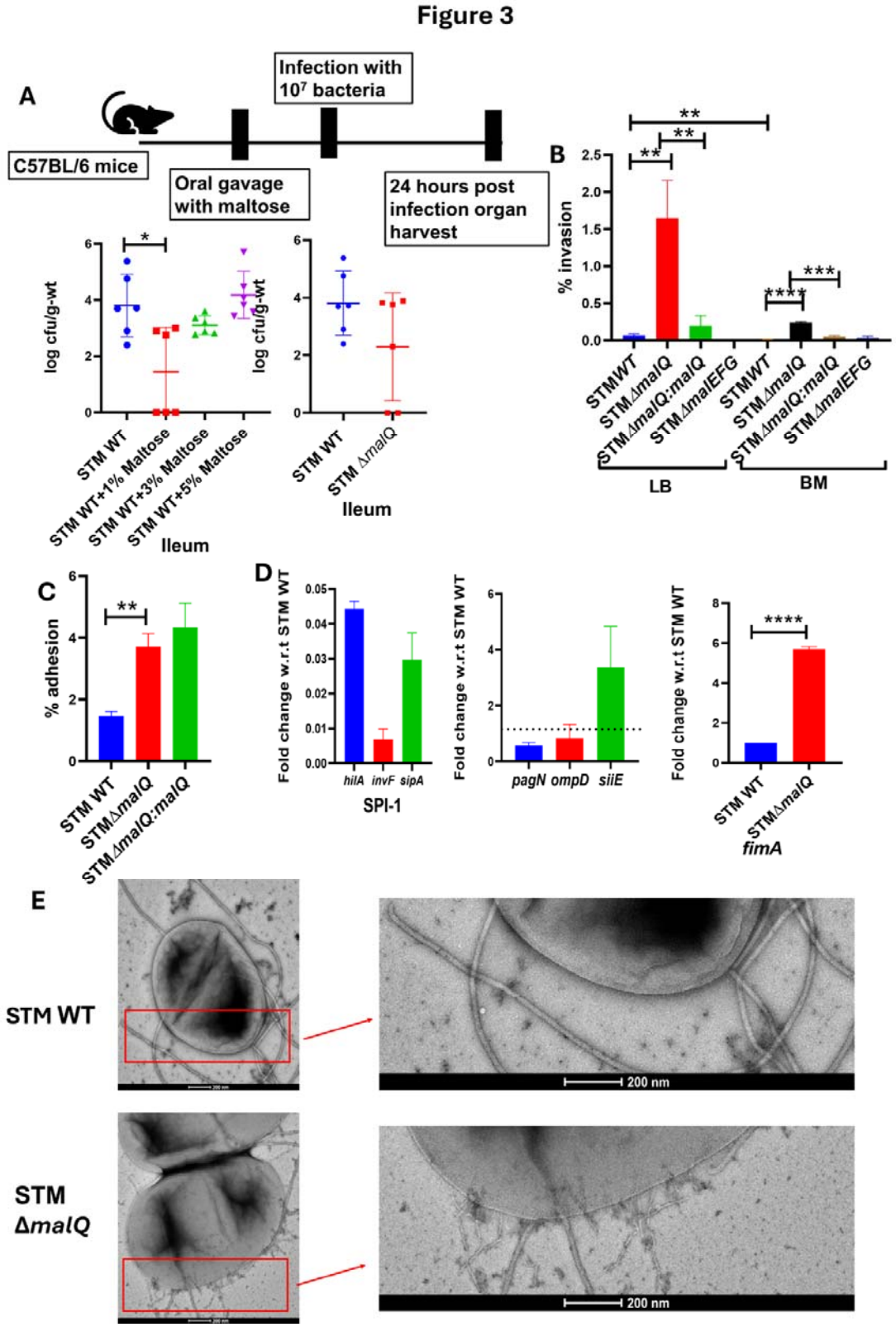

A. Schematic representation of infection and organ burden in the ileum of mice. The Mann- Whitney test was performed for the analysis—six animals per cohort, presented as mean ±SD.

B. Percentage invasion of STM WT, STM Δ*malQ,* STM Δ*malQ:malQ,* STM Δ*malEFG* grown in BM and LB in Caco2 cells. Unpaired Student's t-test was used for the analysis. Data are representative of N=3, n=3, presented as mean ±SD.

C. Percentage adhesion of STM WT, STM Δ*malQ,* STM Δ*malQ:malQ* in Caco2 cells. Unpaired Student's t-test was used for the analysis. Data are representative of N=3, n=3, presented as mean ±SD.

D. mRNA expression of SPI-1 genes (*hilA, invF, sipA),* large proteins (*pagN, ompD, siiE),* and type 1 fimbriae (*fimA)* by q-RT PCR. Unpaired Student's t-test was used for the analysis. Data are representative of N=3, n=3, presented as mean ±SD.

E. Transmission electron microscopy images of STM WT and STM Δ*malQ.*

Figure 4. Type 1 fimbriae mediate the increased adhesion of STM Δ*malQ*.

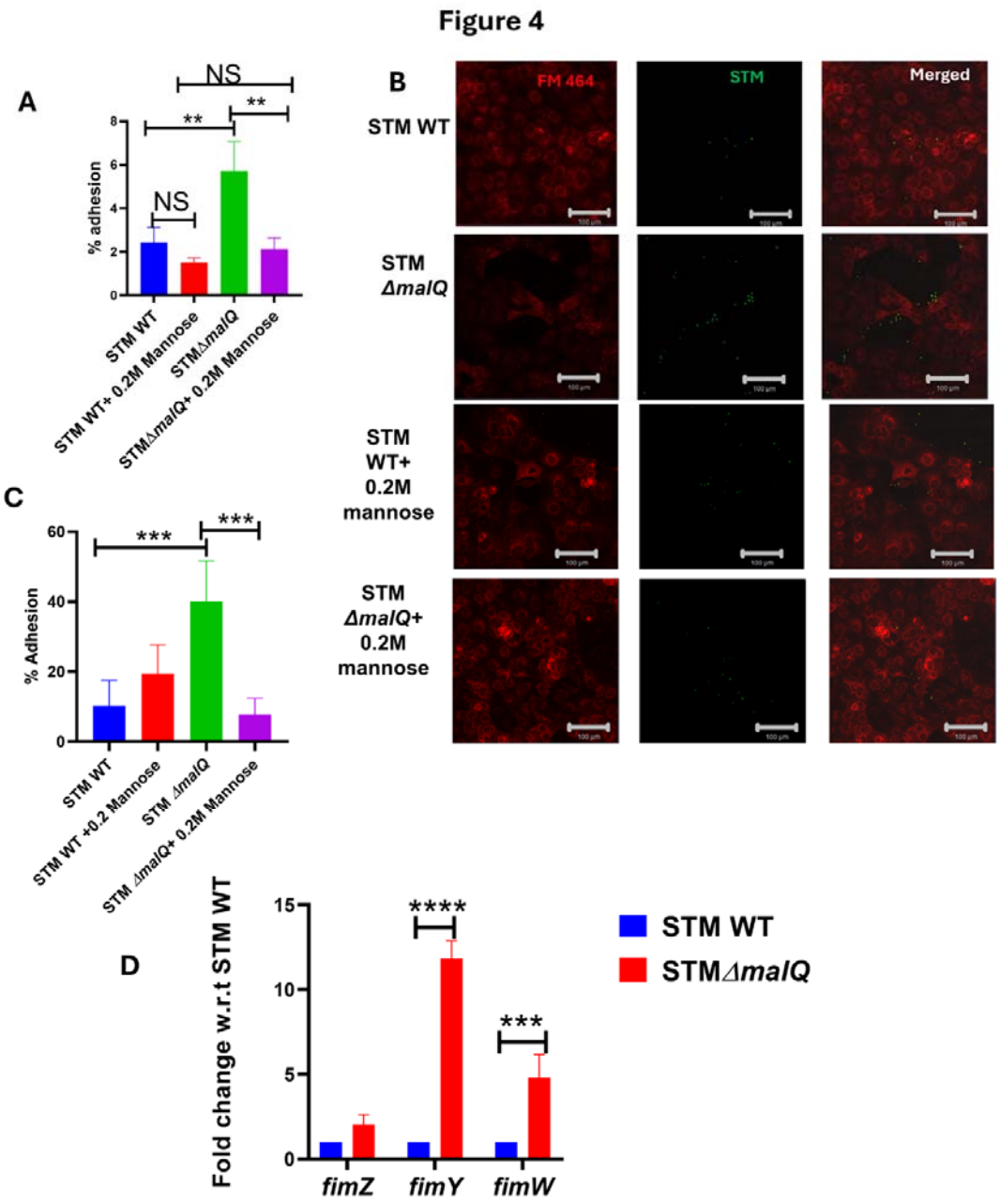

A. The percentage adhesion of STM WT and STM Δ*malQ* in Caco-2 cells treated with and without 0.2 M mannose. One-way ANOVA was used for analysis. Data are representative of N=3, n=3, presented as mean ±SD.

B and C. Confocal microscopy was used to determine the adhesion percentage of STM WT, STM Δ*malQ* in Caco-2 cells on treatment with and without 0.2 M mannose. One-way ANOVA was used for the analysis. Data are representative of N=2, n=5, presented as mean ±SD.

D. mRNA expression of the fimbrial regulatory molecules *fimz, fimY* and *fimW* in STM WT and STM Δ*malQ* by using q-RT PCR. Two-way ANOVA was used for the analysis. Data are representative of N=3, n=3, presented as mean ±SD.

Supplementary information

Supplementary Figure 1. *Salmonella* growth in nitrogen-deficient conditions

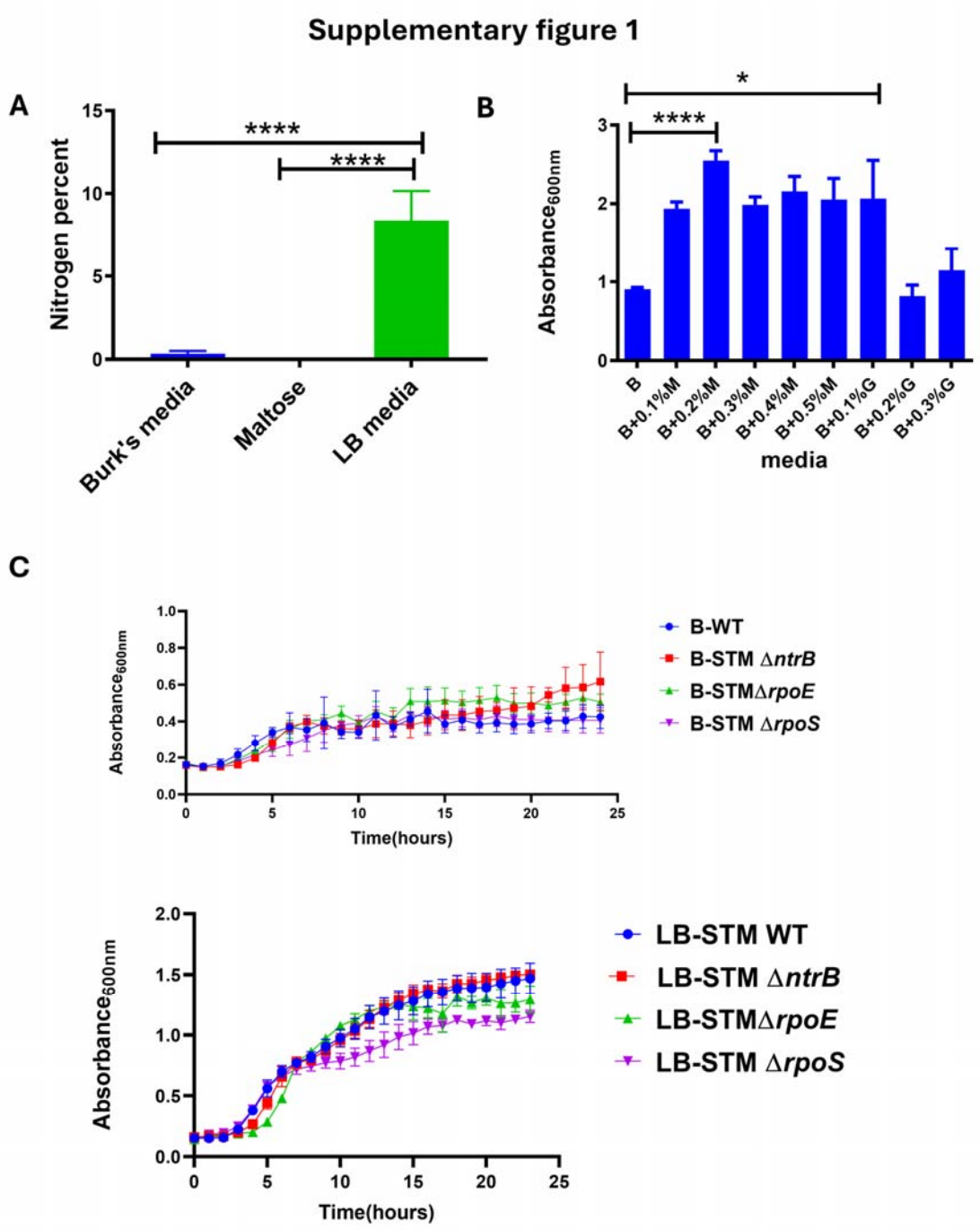

A. CHN analysis was used to determine the nitrogen percentage in Burk's medium, Maltose and LB medium. Unpaired Student's t-test was used for the analysis. Data represents n=6, presented as mean±SD.

B. *Salmonella* Typhimurium growth in Burk's medium with supplementation of glucose and maltose at various concentrations. Unpaired Student's t-test was used for analysis. Data are representative of N=3, n=3, presented as mean ±SD.

C. Growth curve analysis by absorbance of STM WT, STM Δ*ntrB*, STM Δ*rpoE*, STM Δ*rpoS* in Burk's medium and LB medium. Data are representative of N=3, n=5, presented as mean±SD.

Supplementary figure 2. Maltose is responsible for the growth of *Salmonella* in BM conditions.

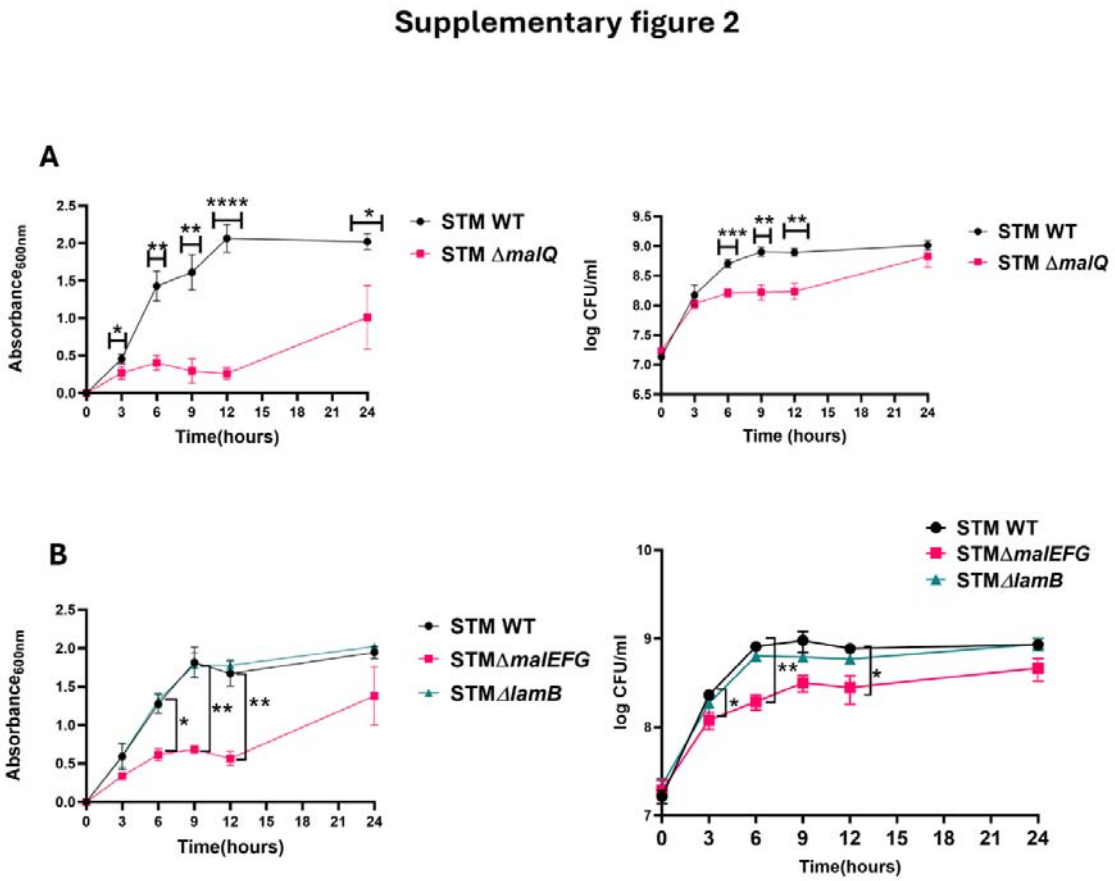

A. Growth curve analysis by absorbance and CFU at various time points of STM WT and STM Δ*malQ*. Unpaired Student's t-test was used for the analysis. Data are representative of N=3, n=2, presented as mean±SD.

B. Growth curve analysis by absorbance and CFU at various time points for STM WT, STM Δ*lamB* and STM Δ*malEFG*. Unpaired Student's t-test was used for the analysis. Data are representative of N=3, n=2, presented as mean±SD.

Supplementary figure 3. Maltose metabolism gene *malQ* helps in the colonisation of mouse model.

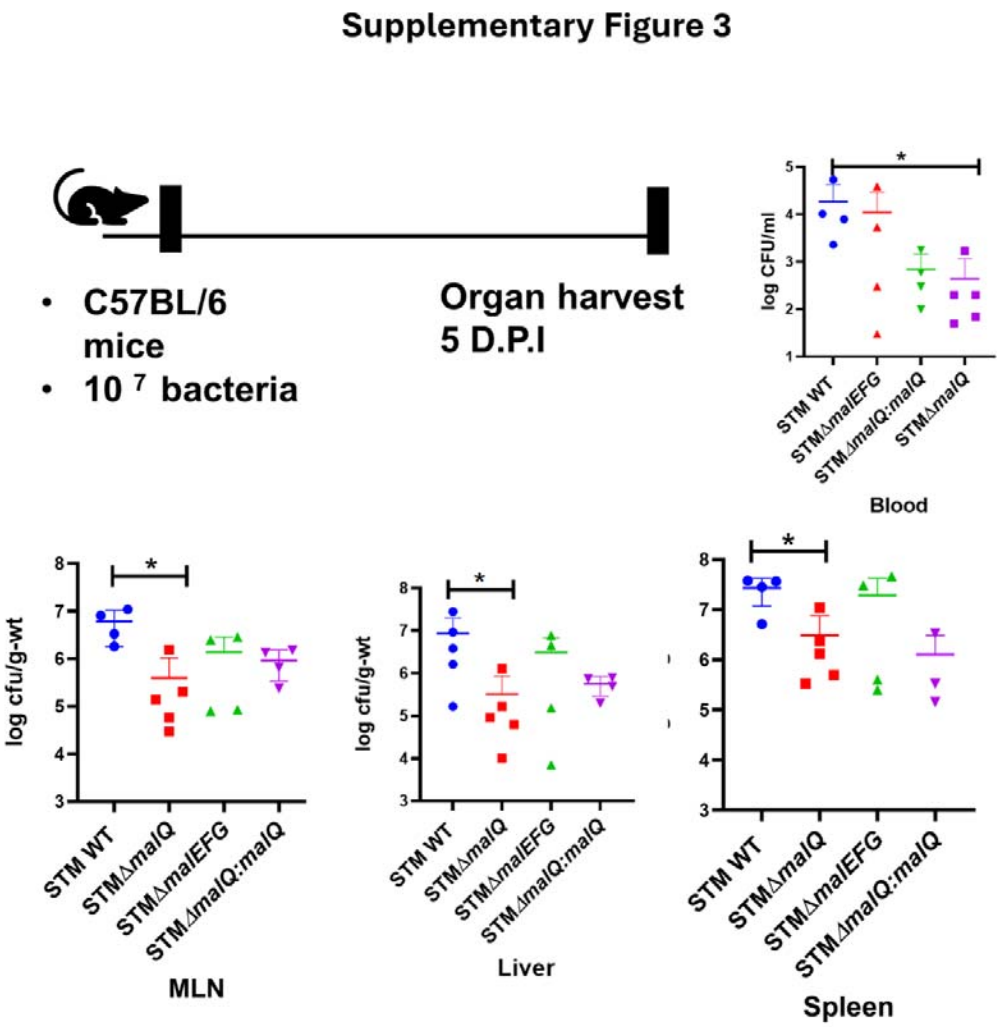

A. *In-vivo* pathogenesis of STM WT, STM Δ*malQ* and STM Δ*malEFG* in C57BL/6 mice post 5 days post infection. Organ burden in blood, MLN, Liver and spleen were determined. The Mann- Whitney test was performed for the analysis—five animals per cohort, presented as mean ±SD.

Supplementary figure 4. Maltose inhibits the biofilm formation of *Salmonella* Typhimurium.

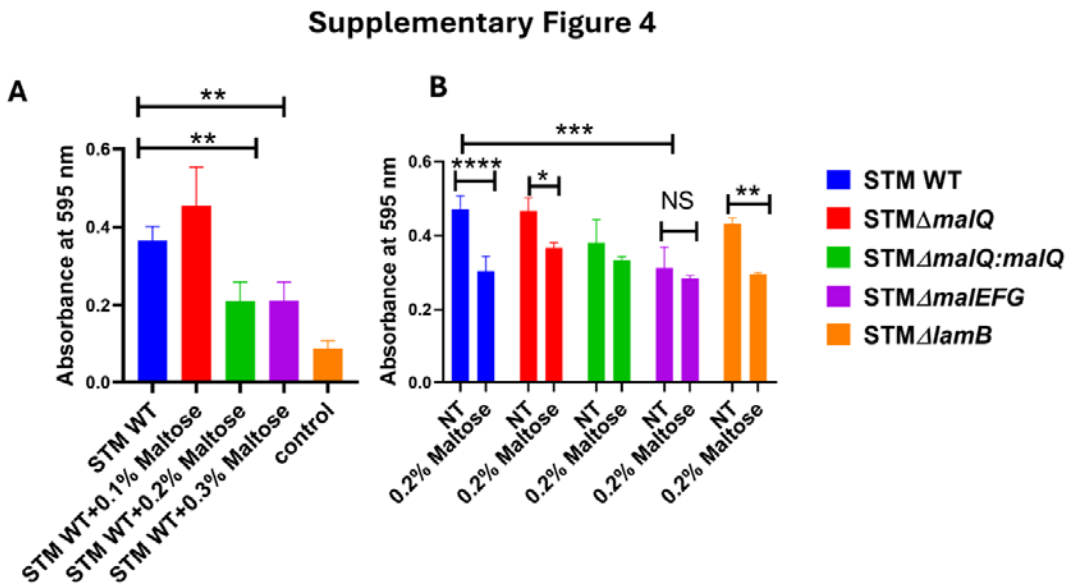

A. Crystal violet staining of the biofilm 3 days post inoculation with different concentrations of maltose. Data is representative of N=3,n=4, presented as mean±SD, analysis by unpaired t-test.

B. Crystal violet staining of the biofilm 3 days post inoculation with STM WT, STM STM Δ*malQ*, STMΔ*malEFG* and STM Δ*lamB* on treatment with and without treatment of 0.2 % maltose. Data is representative of N=3,n=4, presented as mean±SD, analysis by two-way ANOVA.

Supplementary Figure 5. Possible mechanism for type 1 fimbriae regulation

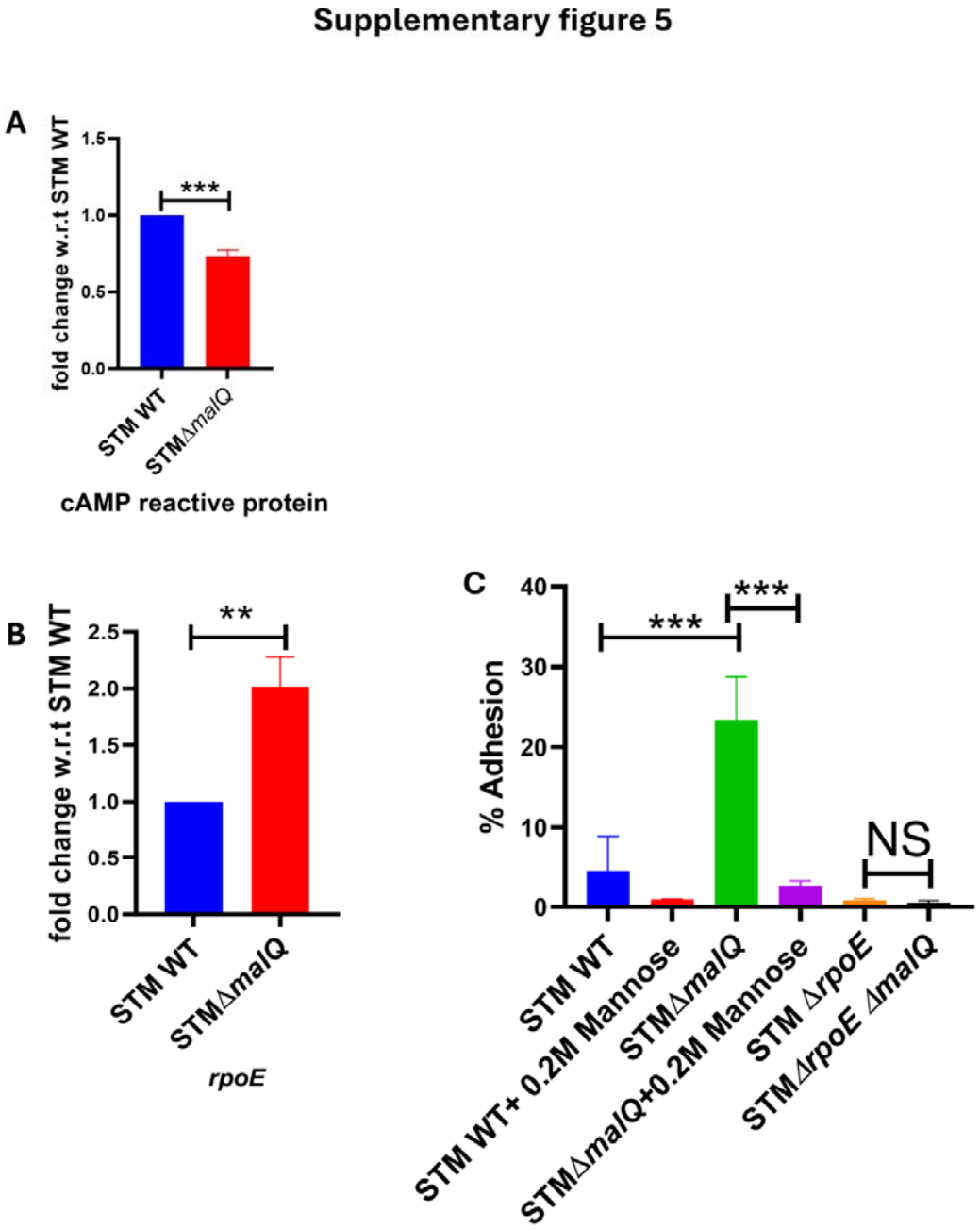

A. mRNA expression of cAMP reactive protein (CRP) in STM WT and STM Δ*malQ* using q-RT PCR. Unpaired Student's t-test was used for analysis. Data are representative of N=3, n=3, presented as mean ±SD.

B. mRNA expression of *rpoE* in STM WT and STM Δ*malQ* using q-RT PCR. Unpaired Student's t-test was used for analysis. Data are representative of N=3, n=3, presented as mean ±SD.

C. Percentage adhesion of STM WT, STM Δ*malQ* in Caco-2 cells on treatment with and without 0.2 M mannose, STMΔ*rpoE* and STMΔ*rpoE* Δ*malQ.* One-way ANOVA was used for the analysis. Data are representative of N=3, n=3, presented as mean ±SD.

Supplementary Table1. List of bacterial strains used in the study

S.NO	Bacterial strain	Antibiotic
1	STM WT 14028S	-
2	STM Δ *ntrB*	Kanamycin
3	STM Δ *malQ*	Kanamycin
4	STM Δ *malEFG*	Kanamycin
5	STM Δ *lamB*	Chloramphenicol
6	STM Δ *malQ: malQ*	Kanamycin :Chloramphenicol
7	STM Δ*rpoS*	Kanamycin
8	STM Δ*rpoE* Δ*malQ*	Kanamycin :Chloramphenicol
9	STM Δ*rpoE (*Made for earlier study) (*46*)	Chloramphenicol

Supplementary Table 2 . List of primers used in the study

Primer name	Sequence
rpoS KO FP	GAACAGCGCTTCGATATTCAGCCCCTGCGTCTGCAGAATT**GTGTAGGCTGGAGCTGCTTC**
rpoS KO RP	GACGCGGAATTTGATGAGAACGGAGTAGAGGCTTTTGACG**CATATGAATATCCTCCTTAG**
rpoS KO Co FP	TATTGATGACGCGCCAATGGT
rpoS KOCo RP	GGAACCAGGCTTTGACTTGC
malQ KO FP	ATGGAAAATAAACGTCTCGATAGTGCCGCGCTGGCGGCGG CATATGAATATCCTCCTTAG
malQ KO RP	TTTCTTCTTCGCGGCCGCTTTTCGGCGTTTATCCAAATCC GTGTAGGCTGGAGCTGCTTC
malQ KO CO FP	GCTCTATTCGCGATTATCAG
*malQ*KO CO RP	GTGCGCCAGGATTGCCTGAT
Comp. *malQ* FP	CCGGAATTCTAAGGGAGCGCGATGGAAAA
Comp. *malQ* RP	CGCGGATCCTCCCCGGCTTTATTATTTCT
ntrB KO FP	TCGGCAGGTAAACCGAAAACTCGGTATGCCCCGGCCAACTGTGTAGGCTGGAGCTGCTTC
ntrB KO RP	ATGGCAAGCGGCATACAGCCCGATGCTGGGCAGATCCTCACATATGAATATCCTCCTTAG
ntrB conf. FP	CGACGACCCAGACTATTCCT
ntrB conf. RP	GCGATGTGACTGGGGTAAGC
malEFG KO FP	GACGACGACATGCGCTGCCATCCTCGCGGAACAGATGACAGTGTAGGCTGGAGCTGCTTC
malEFG KO RP	TCAGGCCGTTGACCAGCCAACGTTGCGCCAACAGGAACACCATATGAATATCCTCCTTAG
malEFG conf. FP	TTCTATCTCCTGAGATCATTGC
malEFG conf. RP	CGACCATAAGTGGGGATAACA
siiE RT FP	GGTCAATGATCATGGCGTGC
siiE RT RP	GTATAGCCCCAGACGCCTTC
fimA RT FP	TTCGGATCGCAGTCATTCAG
fimA RT RP	GTTGCGGCTGATCCTACTC
pagN RT FP	TAGCTTCACATGAGCGAGGC
pagN RT RP	TGAGACGGATGCTAAAGGCG
ompD RT FP	AGTTTGGTGGCGATACCTGG

ompD RT RP	TCATACGTTGCGGACAGACC
16S RT FP	GTGAGGTAACGGCTCACCAA
16S RT RP	TAACCGCAACACCTTCCTCC
hilA RT FP	CGCCGGCGAGATTGTGAGTA
hilA RT RP	TGGCGGAGACACCACTACGA
sipA RT FP	TTCGGATGAAGCGTTGGTCA
sipA RT RP	GTCATTCGCGTGTGGATTCG
rpoE RT FP	GTGCGCTACCAGCATAAAGTG
rpoE RT RP	GCAATACGATACAACCAGGT
cAMP reactive protein FP	TATTGATGACGCGCCAATGGT
cAMP reactive protein RP	TCATCTTTGATCAGCACTGC
fimZ RT FP	GGATGATAGCCGAACAGCGA
fimZ RT RP	TCCGTTTGCGCCCGCTCTTA
fimY FP	ACTCTCCAACGCCGCAGATA
fim Y RP	TGAGCGACCCCTTTTCAATC
fim W FP	ACAGTCACTTTGAGCATGGG
fim W RP	TCAACATCATCTTCCCGAT
rpoE KO FP	GGTTTGGGGAGACATTACCTCGGATGAGCGAGCAGTTACATATGAATA TCCTCCTTAG
rpoE KO RP	CCTAATACCTTTTCCAGTATCCCGCTATCGTCAACGGTGTAGGCTGGAG CTGCTTC
invF RT FP	CGTCGTTTGTGCAGCAGAGC
invF RT RP	TAATTTCCGCGGCGAAACGC